nature cell biology

Wingless promotes cell survival but constrains growth during *Drosophila* wing development

Laura A. Johnston[1,2] and Angela L. Sanders[1]

During animal development, organs grow to a fixed size and shape. Organ development typically begins with a rapid growth phase followed by a gradual decline in growth rate as the organ matures[1], but the regulation of either stage of growth remains unclear. The Wnt/Wingless (Wg) proteins are critical for patterning most animal organs, have diverse effects on development and have been proposed to promote organ growth[2]. Here we report that contrary to this view, Wg activity actually constrains wing growth during *Drosophila melanogaster* wing development. In addition, we demonstrate that Wg is required for wing cell survival, particularly during the rapid growth phase of wing development. We propose that the cell-survival- and growth-constraining activities of Wg function to sculpt and delimit final wing size as part of its overall patterning programme.

The *Drosophila* wing is formed from the wing imaginal disc — a group of epithelial cells that develops in the larva. From its site of synthesis at the dorsal-ventral boundary, Wg patterns the wing disc in a concentration-dependent manner[3,4]. Patterning of the disc is tightly linked to a programme of growth that drives a 1,000-fold increase in cell number over four days. Proliferation of wing disc cells proceeds asynchronously at a rapid rate during the first three days, but slows substantially during the last day, with cells finally arresting in G2 phase at pupariation[5,6]. How this final arrest is regulated is unknown, although it coincides with a pulse of the hormone ecdysone[7,8]. Towards the end of the rapid growth phase, high levels of Wg induce cell cycle arrest in a small subset of cells as part of a regulatory programme resulting in sensory cell differentiation. This zone of non-proliferating cells (ZNCs) flanking the dorsal-ventral boundary arrests approximately 30 h before cells in the rest of the disc[9,10]. Wg induces the arrest in part by inducing expression of proneural fate-specifying genes, which repress expression of the mitotic inducer, *string*^{cdc25} (ref. 10). However, as much evidence indicates that loss of Wg signalling results in reduced wing mass, the prevailing view holds that Wg otherwise promotes wing growth.

We used clonal analysis *in vivo* to measure growth rates during wing development by inducing green fluorescent protein (GFP)-expressing cell clones randomly throughout the wing disc with a 'flp-out' *Gal4* driver[11,12] at precise points spanning disc development. Each clone was allowed to grow for a specific time, allowing the generation of data sets with overlapping growth periods. By counting the number of cells per clone in each data set, we determined how fast cells accumulated within the clone: that is, the clonal growth rate[12]. This growth rate took into account the number of cells that had divided, and those that survived to form a clone within the prescribed time (Fig. 1a). To allow for differences in wing fate, we calculated growth rates separately for clones in the wing pouch, which gives rise to the adult wing blade, and for clones in the surrounding hinge region (Fig. 1b). Growth rates slowed gradually over the course of development, as observed previously by other methods (Fig. 1c)[5]. Hinge cell clones grew faster than wing pouch cells at early (48 h after egg laying (AEL)) and late (115 h AEL) times (Fig. 1c). Taking both wing pouch and hinge clones into account, cell number per clone doubled on average every 9 h during the second and early third instar, but approximately every 13 h at the end of larval development.

To determine how Wg regulates wing growth, we used two approaches to deprive cells of Wg activity. First, we generated cells doubly mutant for the Wg receptors *frizzled1* (*fz1*) and *Dfrizzled 2* (*Dfz2*)[13], or cells mutant for the Wg LRP co-receptor, *arrow* (*arr*)[14], by mitotic recombination using null alleles of these genes. *fz1 Dfz2*$^{-/-}$ mutant cell clones were rarely recovered when induced during the first or early second instar[13]. When induced during the late second or third instar, mutant clones formed, probably through receptor perdurance, although they contained significantly fewer cells than wild-type sister clones generated in the same recombination event (Fig. 2a). Similarly, *arr*$^{-/-}$ cells did not form clones in the wing pouch when mosaics were generated early, although in contrast to *fz1Dfz2*$^{-/-}$ mutants small *arr*$^{-/-}$ clones in the hinge and notum were readily detected (Fig. 2c). Second, we generated GFP-marked clones expressing a dominant negative form of the Wg transducer dTcf/Pangolin (dTcf^{DN}) to block Wg signalling[15]. Similarly to receptor-mutant cells, cell clones expressing dTCF^{DN} grew slowly, particularly in the wing pouch during the second and early third instar (Fig. 1d). dTcf^{DN} had a milder effect on the growth of clones after 96 h AEL in both the wing pouch and hinge cells (Fig. 1d). Because the growth effects of Wg signal deprivation were most marked in the wing pouch, we focused our subsequent analysis on this region of the disc.

Measurements of growth take into account cell division, cellular biosynthesis (cell growth) and cell survival, and changes in any one of

[1]Department of Genetics & Development, College of Physicians & Surgeons Columbia University 701 West 168th Street, New York, NY 10032, USA.
[2]Correspondence should be addressed to L.A.J. (e-mail: lj180@columbia.edu).

Published online: 24 August 2003; DOI: 10.1038/ncb1041

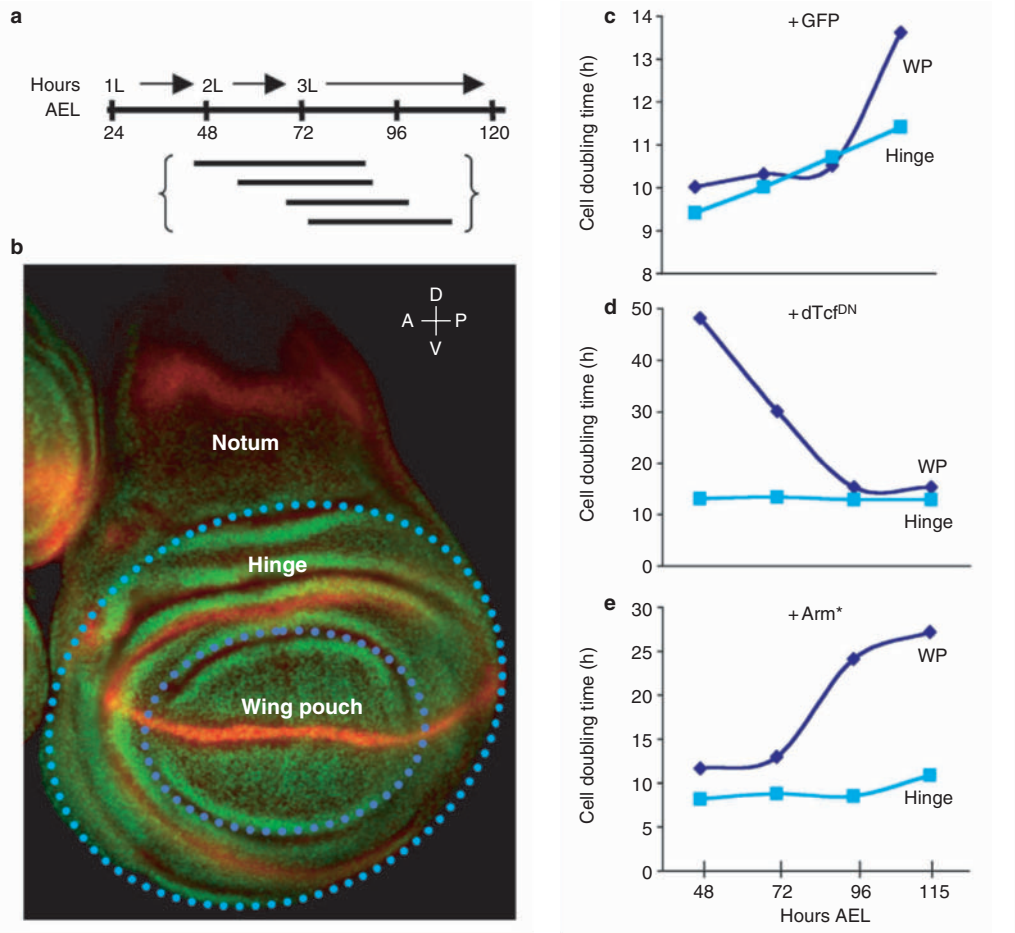

Figure 1 Strategy for analysing growth during wing development. (**a**) Clones of cells were generated according to the strategy depicted. Wing discs develop over 4 days in larvae; a timeline of disc development noting hours after egg laying (AEL) and each larval instar (1L, 2L and 3L) is represented. Horizontal lines in brackets represent the duration of growth per experimental set (clone induction on left, fixation on right) for generation of overlapping sets of clones. (**b**) The wing disc. Wg expression is shown in red; nuclear staining is shown in green. The disc is oriented as described in upper right corner: A, anterior; P, posterior; D, dorsal; V, ventral. Hereafter, all images of discs have this orientation. Clones generated using the strategy described in **a** are scored according to the regions depicted. Hinge cells include dorsal and ventral hinge and pleura (light blue circle). Wing pouch (WP) cells are those within the inner blue circle. Clones in the notum were not scored. (**c**) Cell doubling times of GFP-expressing control clones in the wing pouch and hinge during normal disc development. High numbers correspond to slow growth rates, low numbers to faster growth rates. Note the differing scales on the *y*-axis in **c, d** and **e**. Numbers on the *x*-axis represent approximate mid-point of growth periods. (**d**) Cell doubling times of hinge and wing pouch cell clones expressing $dTcf^{DN}$ to block Wg signalling. Cell doubling times of cells in clones in the wing pouch are significantly longer than in clones in the hinge region, or in wing pouch control clones. (**e**) Cell doubling times of cells in hinge and wing pouch clones expressing Arm* to constitutively activate Wg signalling.

these processes could explain why clones lacking Wg activity grow poorly. Cell death occurs infrequently during normal wing disc development[16], but we repeatedly noticed fragments of DNA and GFP, indicative of cell death, in both the small *fz1Dfz2*$^{-/-}$ clones (Fig. 2e, e′) and cells expressing $dTcf^{DN}$ (Fig. 2i). We confirmed these observations by TUNEL assay (Fig. 2f, g). On the basis of these observations, we blocked apoptosis with the pan-caspase inhibitor P35 (ref. 17) in both *fz1Dfz2*$^{-/-}$ and *arr*$^{-/-}$ mutant clones, and found that clone size was substantially increased, although clones did not reach the size of their siblings because of an approximately 30-h lag before P35 induction (Fig. 2b, d; data not shown). Co-expression of P35 with $dTCF^{DN}$ in cell clones also markedly enhanced their size (Fig. 2j). These results indicate that wing cells deprived of Wg activity die at high frequency, and explain the slow growth rate and small size of the clones. Interestingly, the impact of Wg activity on wing disc cell survival is markedly less during the late third instar than in the second instar, suggesting that Wg signalling is most critical for cell survival during the early, rapid growth, phase of wing development (Fig. 2m, left).

These data suggested that cells deprived of Wg signalling undergo apoptosis, but that the cells proliferate when forced to survive. The elimination of cell death as a factor in clonal growth allowed us to measure how fast these cells were actually dividing. Unexpectedly, we found that cells co-expressing P35 and $dTcf^{DN}$ divided 25% faster than cells expressing P35 alone (compare Fig. 2m, right, with Fig. 2l, right; $P < 001$). Thus, cells forced to survive after removal of Wg activity remain competent to proliferate and do so at a faster rate than normal. As cells deprived of Wg activity divided faster than cells receiving a Wg signal, it seemed possible that Wg normally represses growth rates in

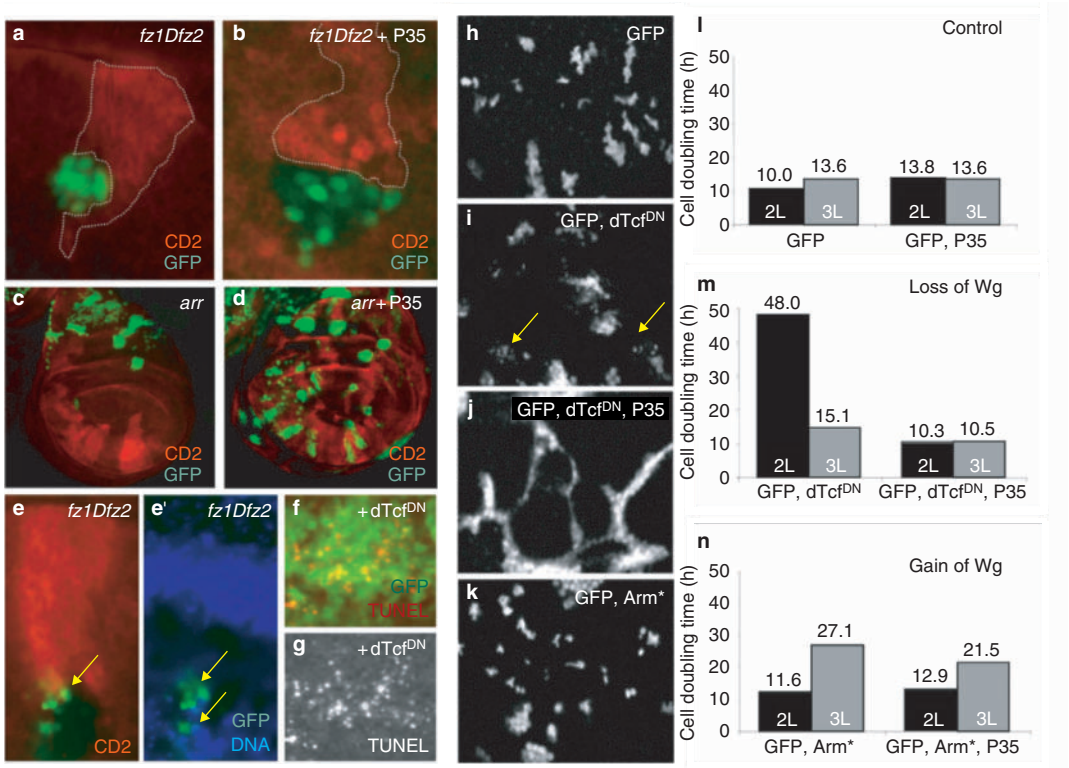

Figure 2 Wing pouch cells deprived of Wg die at high frequency. Panels **a**–**d** show that wing pouch cells deprived of Wg signalling survive poorly, but can be rescued when cell death is blocked. (**a**) A *fz1Dfz2*$^{-/-}$ clone induced during the second instar by MARCM. (**b**) A MARCM GFP-marked *fz*^{1}*Dfz2*$^{-/-}$ clone expressing *P35*, which blocks apoptosis. (**c**) An *arr* mosaic wing disc, showing a large MARCM twin clone (red) with no corresponding *arr* $^{-/-}$ mutant clone. (**d**) When P35 is expressed in *arr*$^{-/-}$ mutant cells (marked with GFP) the clones grow at rates similar to twins. Evidence of cell death in clones lacking Wg activity is shown in panels **e**–**g**. (**e**, **e'**) A MARCM *fz1Dfz2*$^{-/-}$ clone induced during the second instar showing GFP and DNA fragments, indicative of cell death within the clone (arrows). The GFP and DNA fragments are basally positioned in the epithelium, thus in a different focal plane than the twin clone, marked by CD2 (red) in **e**. (**f**, **g**) TUNEL staining, showing dying cells in a disc in which dTcf^{DN} was expressed broadly in the wing pouch. Panel **g** shows a single-channel image of TUNEL staining. Most, but not all, cell death occurs in cells expressing dTcf^{DN}. Panels **h**–**k** show the wing pouch region of wing discs with GFP-expressing cell clones induced at 60 ± 4 h AEL. (**h**) Control clones expressing GFP alone. (**i**) Clones expressing GFP and dTcf^{DN}. Note fragments of GFP, which indicate cell death (arrows). (**j**) Clones expressing GFP, dTcf^{DN} and P35. (**k**) GFP + Arm*-expressing cell clones. In panels **l**–**n**, cell doubling times of cells in clones within the wing pouch are shown. Clones were induced during the second instar and scored 48 h later (black bars, 2L), or during the third-instar and scored 43 h later (grey bars, 3L). (**l**) Control clones expressing GFP alone, or GFP and P35. (**m**) Cell doubling times of cells in clones expressing dTcf^{DN} in the absence (left) or presence (right) of P35. Clones grown during 3L (grey bars) were less affected by cell death. (**n**) Constitutive Wg activity in the wing pouch slows growth rates during 3L. Cell doubling times of cells expressing Arm* and P35, compared with Arm* alone. Cell clones expressing Arm* induced during the second instar (black bars) grew slightly slower than controls (compare with l, GFP); P35 brought these growth rates close to controls (compare with **l**, GFP, P35). When cell death was blocked, Arm*-expressing clones induced during the third-instar (**n**, grey bars, GFP, Arm*, P35) grew 8 h slower than controls (**l**, grey bars, GFP, P35).

the wing pouch. This leads to the prediction that over-activation of Wg signalling will reduce growth rates. Therefore, we expressed a constitutively active form of the Wg transducer, Armadillo/β-catenin (Arm* (ref. 3)), in cell clones and found that during the third instar, Arm*-expressing clones within the wing pouch had many fewer cells than control clones induced in parallel (Figs 1e and 2n). The reduced rate of clonal growth was caused primarily by a slower rate of cell division, as blocking cell death with P35 resulted in cell doubling times that were still 8 h longer than controls expressing P35 alone (21.5 h versus 13.6 h, respectively; Fig. 2n and l, grey bars). Together, the loss- and gain-of-function experiments lead us to conclude that Wg activity constrains growth of the developing wing pouch.

Wg activity is required for the specification of wing pouch cell fates. To make certain that surviving cells lacking Wg activity did not proliferate faster than normal as a result of a switch to non-wing fates, we examined several wing-fate markers. Cells expressing dTcf^{DN}, with or without P35, lost expression of the wing-blade specific gene, *vestigial* (*vg*), as well as *Distalless* (*Dll*), both of which are targets of Wg signalling (data not shown and see Supplementary Information, Fig. S1). The cells seem to maintain wing pouch identity, however, as the Pdm-1 protein Nubbin (Nub)[18] was still expressed in wing pouch cells expressing dTcf^{DN} (see Supplementary Information, Fig. S1d). Furthermore, expression of the hinge-specific proteins Homothorax (Hth) and Teashirt (Tsh)[19,20] remained restricted to hinge regions (see Supplementary Information, Fig. S1c, d), demonstrating that the cells did not acquire proximal wing fates. These observations suggest that despite losing *vg* expression, cells forced to survive after Wg deprivation retained wing fates. Interestingly, co-expression of either a *Vg* or *Dll* transgene with dTcf^{DN} was not sufficient to overcome the growth and survival defects of Wg deprivation (see Supplementary Information, Table 1).

Next, we explored the basis for the negative effect of Wg on wing pouch growth by examining the cell cycles of cells in which Wg activity was modulated. Analysis of specific cell cycle regulatory factors identified a

temporal 'growth profile' that reflected the developmental maturity of the wing disc. dE2F1 is a transcription factor that regulates expression of several genes necessary for cell cycle progression, including *stg*^{cdc25} (refs 12, 21). By monitoring dE2F1 activity using an dE2F1-responsive reporter[22], and *stg*^{cdc25} expression by RNA *in situ* hybridization, we found that both were regulated in the wing disc in an age-dependent manner: we observed strong expression and activity in young wild-type discs, which declined as the disc matured during pupariation (Fig. 3a–f). We also used flow cytometry to track the cell cycles of wing disc cells (Fig. 4a, b)[12]. Immature, rapidly cycling, wing disc cells spent most of each cell cycle in G1 phase, and less time in S phase and G2/M (Fig. 4a). As discs matured and cell cycles slowed during the third instar, phasing was reversed with cells spending less time in G1 and more of the total cycle in G2 (Fig. 4b). Thus, temporal changes in growth during wing development can be followed with this characteristic growth profile.

When Wg signalling was modulated, the normal spatial and temporal regulation of dE2F1 and *stg*^{cdc25} was disrupted. Loss of Wg activity (dTcf^{DN} + P35) resulted in increased dE2F1 activity (Fig. 3g) and *stg*^{cdc25} mRNA levels (Fig. 3i). Parallel experiments in which P35 was expressed alone did not result in any of these changes (data not shown[12]). In contrast, gain of Wg activity with either an *Arm** or a *Wg* transgene decreased dE2F1 activity (Fig. 3h and see Supplementary Information, Fig. S2) and resulted in significantly lower levels of *stg*^{cdc25} mRNA than in control discs of the same developmental age (Fig. 3j). The molecular deregulation was mirrored by the cell cycle distribution. Cells co-expressing dTcf^{DN} and P35 cycled out of phase with internal control cells from the same discs, spending more time in G1 and less time in G2 (Fig. 4d). The cell cycle distribution resulting from loss of Wg signalling was strikingly similar to that of cells from immature wing discs. In addition, the 'immature' cell cycle distribution induced by dTcf^{DN} occurred even in older wing discs when non-expressing cells in the same disc cycled with mature phasing appropriate for their age (Fig. 4d). Expression of Arm* also caused cells to cycle aberrantly, compared with internal control cells. Arm*-expressing cells had cell cycle phasing characteristic of mature wing disc cells, rather than phasing appropriate for their chronological age (Fig. 4f). The 'mature' cell cycle phasing was observed 24 h after the onset of Arm* expression. These alterations in phasing were accompanied by either a faster (loss of Wg activity) or slower (gain of Wg activity) cell cycle length (Fig. 2l–n). Gain or loss of Wg signalling did not significantly alter cell size in any of these experiments (Fig. 4c–f). As cell size can reflect how fast cellular biosynthesis proceeds during each cell division cycle, we conclude that Wg regulates rates of cellular biosynthesis and cell division coordinately.

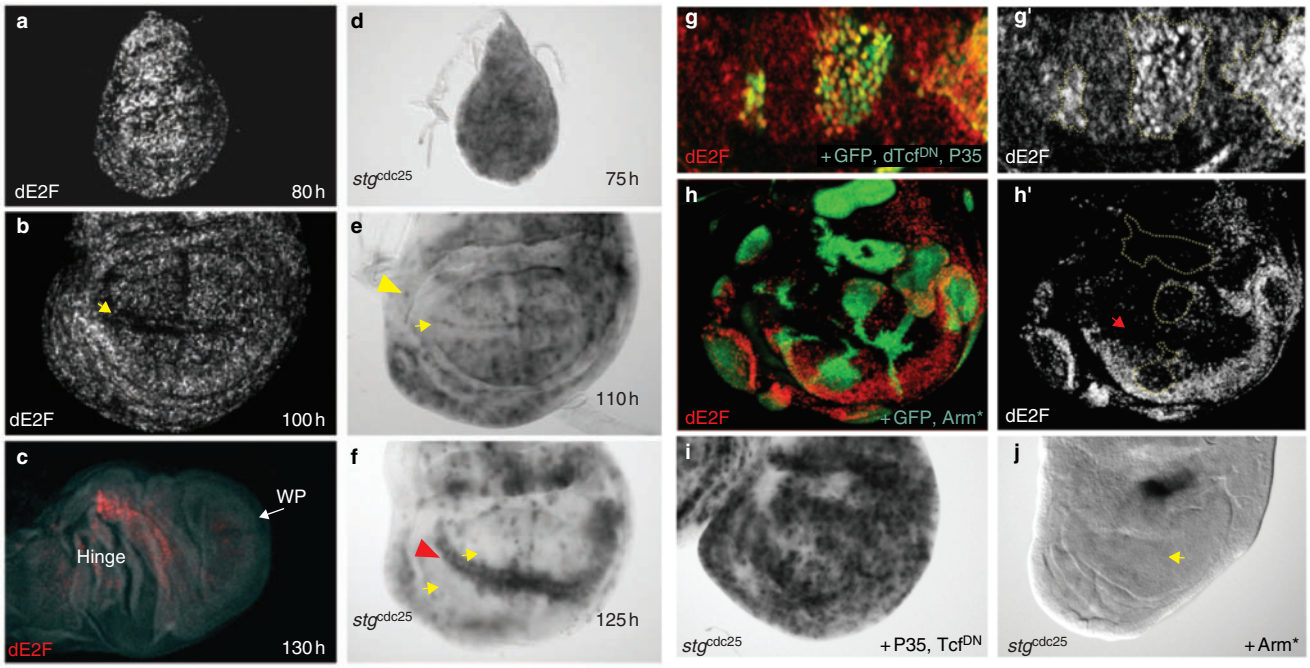

Figure 3 Altering Wg activity disrupts the growth profile. Panels **a–c** show that dE2F1 activity is high in immature discs and declines as the disc ages. Control discs 80, 100 and 130 h AEL, showing pattern of dE2F1 activity from the activity reporter[22]. Arrow in **c** points to the wing pouch. Note the proximal–distal axis is oriented vertically in this image, as the wing pouch is beginning to evert. Panel **b** shows that although dE2F1 activity is present in many cells of the disc, it is excluded from others at this stage, including the ZNC (arrow). Panel **c** shows that at pupariation, dE2F1 activity (red) is almost entirely lost in wing pouch cells but is still present in hinge cells. (**d–f**) *stg*^{cdc25} mRNA expression during wing development 75, 110 and 125 h AEL (white prepupal stage). *stg*^{cdc25} expression is lost from specific groups of sensory precursor cells: for example, proximal and distal costal cells (arrowhead in **e**), and anterior cells of the ZNC (arrow in **e**). As larval development ends, *stg*^{cdc25} expression is re-expressed in all cells of the ZNC (arrowhead in **f**), whereas expression has declined in most cells of the wing pouch (arrows in **f**). (**g**, **g′**) dE2F1 activity is considerably higher in cell clones (outlined in **g′**) in the wing pouch expressing dTcf^{DN} and P35 (marked by GFP in **g**) than in the rest of the disc. (**h**, **h′**) In the wing pouch, dE2F1 activity is reduced in cell clones (outlined in **h′**) expressing Arm* (marked with GFP in **h**). Note that at the edges of the outlined clones some dE2F1 activity remains, suggesting a non-autonomous effect on dE2F1 activity induced by the interface between WT and Arm*-expressing cells. Cells in the ZNC (arrow) have no dE2F activity because of cell cycle arrest[10]. (**i**) A late third-instar wing disc expressing dTcf^{DN} and P35 in the wing pouch. Cells expressing dTcf^{DN} and P35 continue to express *stg*^{cdc25}. Discs were staged according to morphology, as these larvae are developmentally delayed (approximately 1.5 days); this disc is comparable developmentally with the disc in **f.** (**j**) *stg*^{cdc25} is repressed by Arm* expression throughout the wing pouch in late third-instar wing discs. Staining above the wing pouch is *stg*^{cdc25} mRNA in hinge cells.

Our data argue that the changes in regulation of dE2F1 and *stg*^{cdc25} resulting from loss or gain of Wg activity result in altered cell cycle phasing of the cells and ultimately to altered rates of cell division. We tested the requirement for dE2F1 activity in Wg-mediated regulation of cell proliferation by co-expressing the dE2F1 inhibitor, RBF, which slows cell division rates[12], along with dTcf^{DN} and P35. Under these conditions, the clones contained very few cells (mean = 3 ± 2; n = 30), indicating that RBF slowed cell proliferation in surviving cells that lack Wg activity (data not shown). In addition, co-expression of dE2F1 and Arm* resulted in faster cell doubling times than Arm* alone (10.8 h (n = 52) versus 26.5 h (n = 28), respectively). These data are consistent with a model in which Wg regulates cell proliferation rates by suppressing dE2F1 activity.

Wg directs wing patterning through a long-range, concentration-dependent mechanism, such that *vg* and *Dll* are expressed in cells in response to low concentrations of Wg, whereas expression of the proneural genes at the dorsal-ventral boundary requires high levels of Wg[3,4]. The cell cycle arrest of the ZNC, which flanks the dorsal-ventral boundary, also requires Wg and proneural gene function[10]. Here, we find that increasing Wg activity in cells in which endogenous levels of Wg are relatively low does not cause their arrest, but results in a slower rate of cell proliferation, reduced expression of *stg*^{cdc25} and low dE2F1 activity. These observations suggest the possibility that different thresholds of Wg signalling in the wing pouch elicit different growth outcomes. In support of this idea, expression of Arm* with a strong *Gal4* driver imposed high levels of Wg activity in the wing pouch, illustrated by the widely expanded domain of cells expressing Senseless (Sens), a proneural marker[23] (Fig. 4i), and broad repression of *stg*^{cdc25} mRNA expression (see Fig. 3j for example). Conversely, when a moderate level of Wg activity was induced by using the same driver to express a Wg transgene, *stg*^{cdc25} expression was reduced, but not entirely absent, and cell cycles with extended G2 phases were induced (Fig. 4e, f and data not shown). Under these conditions, Sens expression was restricted to cells in close proximity to the dorsal-ventral boundary, where endogenous Wg was expressed at high levels (Fig. 4h). These data suggest that similarly to the patterning read-outs, the growth read-outs of Wg activity are concentration-dependent: the high concentration of Wg at the dorsal-ventral boundary induces Sens and a complete loss of *stg*^{cdc25}, and may contribute to the arrest of those cells. In contrast, moderate levels merely reduce *stg*^{cdc25} expression and slow cell proliferation rates.

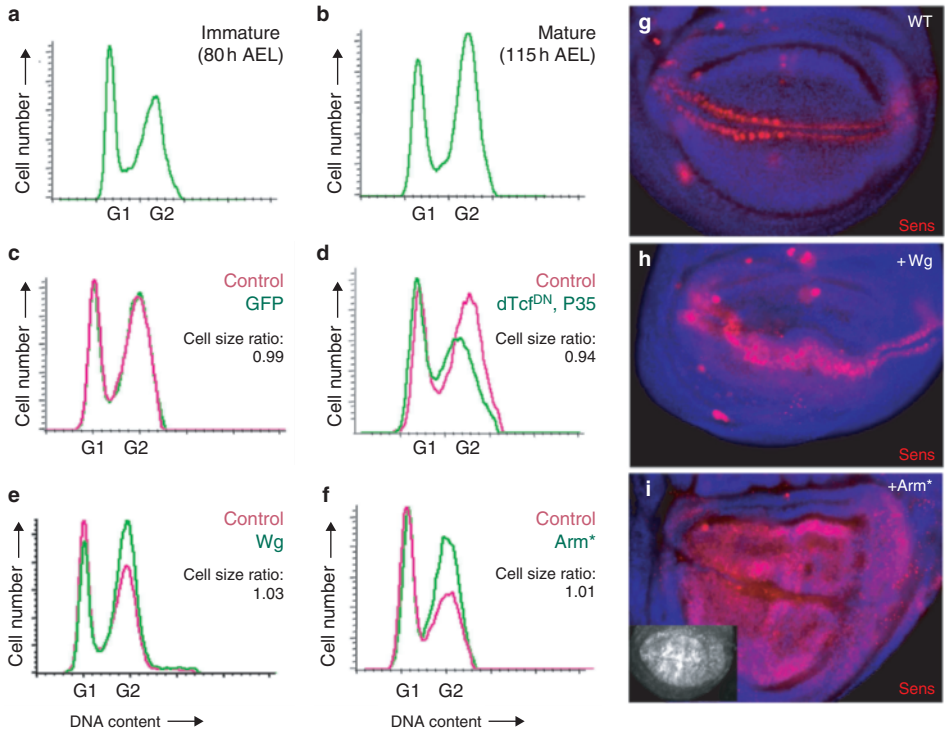

Figure 4 Loss or gain of Wg alters cell cycle phasing. (**a**–**f**) Cell cycle profiles of wing disc cells analysed by flow cytometry. Green trace represents the GFP-positive experimental cells; red trace represents the GFP-negative internal control cells. Wing discs in **c**–**e** were processed for flow cytometry at 110 ± 2 h AEL; discs in **f** were processed at 96 ± 2 h AEL. Panel **a** shows a typical cell cycle profile of a wing disc from the early third-instar (80 h AEL). Panel **b** shows the cell cycle profile from a mature wing disc (115 ± 2 h AEL). Panel **c** shows that the cell cycle profiles of control clones expressing GFP (green trace), or GFP and P35 (data not shown), are identical to that of internal control cells within the same disc (red trace). Panel **d** shows that cells co-expressing dTcf^{DN} and P35 (green) display a cell cycle profile characteristic of immature cells (compare with **a**), whereas internal control cells within the same disc transit the cycle with a DNA profile characteristic of their chronological age (110 ± 2 h AEL). (**e**, **f**) Cells expressing either *Wg* or *Arm** transgenes assume a 'mature' DNA profile (green trace, compare with **b**), even while the phasing of internal control cells (red trace) is younger, appropriate to the age of the disc (96 ± 2 h AEL). (**g–i**) A mature growth profile and loss of *stg*^{cdc25} is not strictly correlated with proneural gene expression. Panel **g** shows that in late third-instar wing discs, Sens is expressed in two stripes flanking the dorsal-ventral boundary. Panel **h** shows that moderate levels of Wg signal activation, through expression of Wg throughout the wing pouch, results in limited expansion of Sens expression. Panel **i** shows that high-level Wg activation with Arm* expression results in significant expansion of Sens expression dorsally and ventrally, and that *stg*^{cdc25} expression is completely lost in those cells (Fig. 3j). Both Wg and Arm* were expressed with the same Gal4 driver (C765), shown in the inset in **i** (expression domain marked with GFP).

Taken together, our data demonstrate that surviving cells deprived of Wg signalling acquire an immature-like growth state, whereas with increased Wg signalling cells assume a more developmentally mature growth state. These observations imply that Wg controls the timing of the growth maturation of wing disc cells through its regulation of key cell cycle regulatory factors. As increasing Wg activity resulted in significant slowing of clonal growth only during the third instar (Figs 1e and 2n), we infer that the final maturation of the wing disc growth profile by Wg requires some earlier gating function or developmental 'priming'; for example, the acquisition of certain cell fates. Given that cell cycle arrest of the ZNC is achieved through activation of Wg target genes[10], we speculate that growth maturation of the disc is also controlled indirectly.

We have demonstrated that during the rapid growth phase of immature wing discs, Wg promotes cell survival and keeps growth rates in check while it patterns wing-specific fates. The pro-apoptotic gene *hid* is upregulated in cells lacking Wg activity (data not shown), and *hid* mutants dominantly suppress *armadillo* mutant embryos[24], suggesting that Wg may directly or indirectly promote cell survival by regulating *hid* expression. Our data indicate that when wing patterning is almost complete, Wg activity provides an increasing brake on growth by enforcing a decline in key cell cycle and growth regulatory factors. The decline in growth rate during organ maturation is of critical importance as it defines the final size of the organ, but its regulation has remained obscure[1]. We propose that Wg activity controls final wing size by regulating the decline in its growth rate at the end of larval development. However, not all tissues respond to Wg by slowing their growth, as hinge cells of the wing disc accelerate growth when Wg activity is increased, resulting in massive overgrowth (Fig. 1e and data not shown). Similarly, Wnt signalling promotes growth in several vertebrate tissues, and in colorectal cancer cells β-catenin/Tcf-4 promotes proliferation of progenitor cells[25]. Our results demonstrate the importance of timing and developmental context in growth instructions from Wg, and add to the diverse array of outcomes regulated by Wnt/Wg signalling. □

METHODS

Fly strains and husbandry. The following strains were used: *w*; *Sp/CyO*; *Act>CD2>Gal4*, *UAS-GFP*[12,26]. *ywflp*; *Sp/CyO*; *UAS-Arm ΔN* (*Arm**)[3]. *ywflp*; *UAS-dTcf*^{DN} (ref. 15). *ywflp*; *UAS-P35*; *UAS-dTcf*^{DN}. *ywflp*; *UAS-P35* (ref. 17). *ywflp*; *UAS-Wg* (B. Sanson). *ywflp*; *arr*^{2} *FRT42D/CyO*[14]. *ywflpUAS-GFP*; *FRT42D TubGal80 y +hsCD2*; *C10Gal4* (G. Struhl). *ywflp*; *UAS-P35/CyO*; *fz1Dfz2 FRT2A/TM6B*[13]. *ywflp TubGal4,UAS-GFP*; *Sp/CyO*; *hsCD2 TubGal80 FRT2A* (G. Struhl). *w*; *C765Gal4*, *UAS-GFP/TM6B*[27]. *yw*; *C96Gal4*, *UAS-GFP*[10]. *w*; *UAS-GFP/CyO*; *AH658Gal4/TM2* (G. Morata). *w*; *MA24* (*Orc1Pr-ftz–GFP–Myc*)[22]. Embryos from appropriate crosses were collected on grape plates for short periods (1–4 h); after hatching ≤ 50 larvae were transferred to yeasted food vials and raised at 25 °C.

Cell proliferation rate measurements. The Flp-out Gal4 cassette was used to generate random clones of cells that express GFP as a lineage marker and other *UAS*-transgenes of interest[11,12,28]. Larval heat shocks to activate Flp recombinase expression were performed at 37 °C for 20 min, at the following times: clones were initiated at the second instar (40, 48 or 60 h AEL) or third instar (72 or 96 h AEL) and allowed to grow for the prescribed times. The location of each clone in the disc was recorded as either hinge or wing pouch, as defined in Fig. 1b. If possible, more than 100 clones were scored per time interval. Cell doubling times were determined by counting the number of cells in each clone after fixing wing discs at the end of the growth period (Fig. 1a), and calculated using the formula log 2 (h)/log N, where N = median cell number/clone, and h = age of the clone. Student's *t*-tests were used to determine significance.

Flow cytometry. Expression of *UAS*-transgenes was induced with a strong larval heat shock (37 °C for 1–2 h) 36–48 h before disc dissociation to get a population of approximately 50% GFP^{+} cells[12,28], and analysis of cell cycle phasing and cell size (by forward scatter) was performed with a FACS Vantage 2 (Becton Dickinson, San Jose, CA) or an Ultra Hypersort (Beckman Coulter, Miami, FL)[12,28]. 20–30 wing discs were examined per experiment. At least five experiments were performed for each genotype. Data analysis was performed with CellQuest (BD) software. Modfit (Verity, Turramurra, NSW) software was used to integrate peak areas and define the fraction of cells in each cell cycle phase.

Histology. Fixation, RNA *in situ* hybridization and immunocytochemistry were performed as described[10]. TUNEL assays were performed using ApopTag (Serologicals, Norcross, GA). Hoechst 33258 (Sigma, St Louis, MO) was used to label DNA. Images were acquired using Openlab software and an Axioplan 2 microscope (Zeiss, Thornwood, NJ) equipped with an Orca-100 CCD camera (Hamamatsu, Hamamatsu City, Japan) and processed with Adobe Photoshop. The following antibodies and dilutions were used: guinea pig-anti-Hth (1:500) and Rat-anti-Tsh (1:200; gifts of R. Mann), mouse-anti-Nub (1:50; gift of S. Cohen), rabbit-anti-Vg (1:500; gift of S. Carroll), mouse-anti-Brdu (1:100; Becton Dickinson), mouse-anti-c-Myc (1:100; Oncogene Sciences, Boston, MA), mouse-anti rat CD2 (1:400; Serotec, Oxford, UK), guinea pig-anti Sens (1:500; H. Bellen). Secondary antibodies were purchased from Jackson Immunoresearch (West Grove, PA) and Molecular Probes (Eugene, OR).

Mitotic recombination. The MARCM (mosaic analysis with a repressible marker) system was used to induce mitotic recombination while positively marking mutant cells with *UAS-GFP*, and to express *UAS-P35* in mutant cells[29].

Note: Supplementary Information is available on the Nature Cell Biology website.

ACKNOWLEDGEMENTS

L.A.J. very gratefully acknowledges the continual encouragement and generous support of Bruce Edgar, in whose lab this work was started. We thank K. Shah, E. Yoshida and L. Gatto for technical assistance, T. Jessel and I. Schieren for FACS use and assistance, and B. Edgar, I. Greenwald, T. Jessel, R. Mann, G. Struhl, A. Tomlinson, and members of the Johnston lab for comments on the manuscript. This work was supported in part by the V Foundation for Cancer Research, NY Speaker's Fund for Biomedical Sciences (L.A.J.) and the National Institutes of Health (HD42770 to L.A.J, GM51186 to B. Edgar). L.A.J. is a V Foundation Scholar.

COMPETING FINANCIAL INTERESTS

The authors declare that they have no competing financial interests.

Received 3 July 2003; accepted 5 August 2003
Published online at http://www.nature.com/naturecellbiology

1. Bryant, P. J. & Simpson, P. Intrinsic and extrinsic control of growth in developing organs. *Q. Rev. Biol.* **59,** 387–415 (1984).
2. Serrano, N. & O'Farrell, P. H. Limb morphogenesis: connections between patterning and growth. *Curr. Biol.* **7,** 186–195 (1997).
3. Zecca, M., Basler, K. & Struhl, G. Direct and long-range action of a wingless morphogen gradient. *Cell* **87,** 833–844 (1996).
4. Neumann, C. J. & Cohen, S. M. Long-range action of Wingless organizes the dorsal–ventral axis of the *Drosophila* wing. *Development* **124,** 871–880 (1997).
5. Bryant, P. J. & Levinson, P. Intrinsic growth control in the imaginal primordia of *Drosophila*, and the autonomous action of a lethal mutation causing overgrowth. *Dev. Biol.* **107,** 355–363 (1985).
6. Garcia-Bellido, A. & Merriam, J. R. Parameters of the wing imaginal disc development of *Drosophila melanogaster*. *Dev. Biol.* **24,** 61–87 (1971).
7. Fain, M. J. & Stevens, B. Alterations in the cell cycle of *Drosophila* imaginal disc cells precede metamorphosis. *Dev. Biol.* **92,** 247–258 (1982).
8. Graves, B. & Schubiger, G. Cell cycle changes during growth and differentiation of imaginal leg discs in *Drosophila melanogaster*. *Dev. Biol.* **93,** 104–110 (1982).
9. O'Brochta, D. A. & Bryant, P. J. A zone of non-proliferating cells at a lineage restriction boundary in *Drosophila*. *Nature* **313,** 138–141 (1985).
10. Johnston, L. A. & Edgar, B. A. Wingless and Notch regulate cell-cycle arrest in the developing *Drosophila* wing. *Nature* **394,** 82–84 (1998).
11. Struhl, G. & Basler, K. Organizing activity of Wingless protein in *Drosophila*. *Cell* **72,** 527–540 (1993).
12. Neufeld, T., de la Cruz, A. F., Johnston, L. A. & Edgar, B. A. Coordination of growth and cell division in the *Drosophila* wing. *Cell* **93,** 1183–1193 (1998).
13. Chen, C. M. & Struhl, G. Wingless transduction by the Frizzled and Frizzled2 proteins of *Drosophila*. *Development* **126,** 5441–52 (1999).
14. Wehrli, M. *et al. arrow* encodes an LDL-receptor-related protein essential for Wingless signalling. *Nature* **407,** 527–530 (2000).
15. van de Wetering, M. *et al.* Armadillo coactivates transcription driven by the product of the *Drosophila* segment polarity gene *dTCF*. *Cell* **88,** 789–799 (1997).
16. Milan, M., Campuzano, S. & Garcia-Bellido, A. Developmental parameters of cell

death in the wing disc of *Drosophila*. *Proc. Natl Acad. Sci. USA* **94,** 5691–5696 (1997).
17. Hay, B. A., Wolff, T. & Rubin, G. M. Expression of baculovirus P35 prevents cell death in *Drosophila*. *Development* **120,** 2121–2129 (1994).
18. Cifuentes, F. J. & Garcia-Bellido, A. Proximo-distal specification in the wing disc of *Drosophila* by the *nubbin* gene. *Proc. Natl Acad. Sci. USA* **94,** 11405–11410 (1997).
19. Azpiazu, N. & Morata, G. Function and regulation of homothorax in the wing imaginal disc of *Drosophila*. *Development* **127,** 2685–2693 (2000).
20. Casares, F. & Mann, R. S. A dual role for homothorax in inhibiting wing blade development and specifying proximal wing identities in *Drosophila*. *Development* **127,** 1499–1508 (2000).
21. Du, W., Xie, J. & Dyson, N. Ectopic expression of dE2F and dDP induces cell proliferation and death in the *Drosophila* eye. *EMBO J.* **15,** 3684–3692 (1996).
22. Asano, M. & Wharton, R. P. E2F mediates developmental and cell cycle regulation of ORC1 in *Drosophila*. *EMBO J.* **18,** 2435–2448 (1999).
23. Nolo, R., Abbott, L. A. & Bellen, H. J. *Drosophila Lyra* mutations are gain-of-function mutations of senseless. *Genetics* **157,** 307–15 (2001).
24. Cox, R. T. *et al.* A screen for mutations that suppress the phenotype of *Drosophila* armadillo, the β-catenin homolog. *Genetics* **155,** 1725–1740 (2000).
25. van de Wetering, M. *et al.* The β-catenin–TCF-4 complex imposes a crypt progenitor phenotype on colorectal cancer cells. *Cell* **111,** 241–250 (2002).
26. Pignoni, F. & Zipursky, S. Induction of *Drosophila* eye development by decapentaplegic. *Development* **124,** 271–278 (1997).
27. Nellen, D., Burke, R., Struhl, G. & Basler, K. Direct and long-range action of a DPP morphogen gradient. *Cell* **85,** 357–368 (1996).
28. Johnston, L. A., Prober, D. A., Edgar, B. A., Eisenman, R. N. & Gallant, P. *Drosophila* Myc regulates cellular growth during development. *Cell* **98,** 779–790 (1999).
29. Lee, T. & Luo, L. Mosaic analysis with a repressible cell marker for studies of gene function in neuronal morphogenesis. *Neuron* **22,** 451–461 (1999).

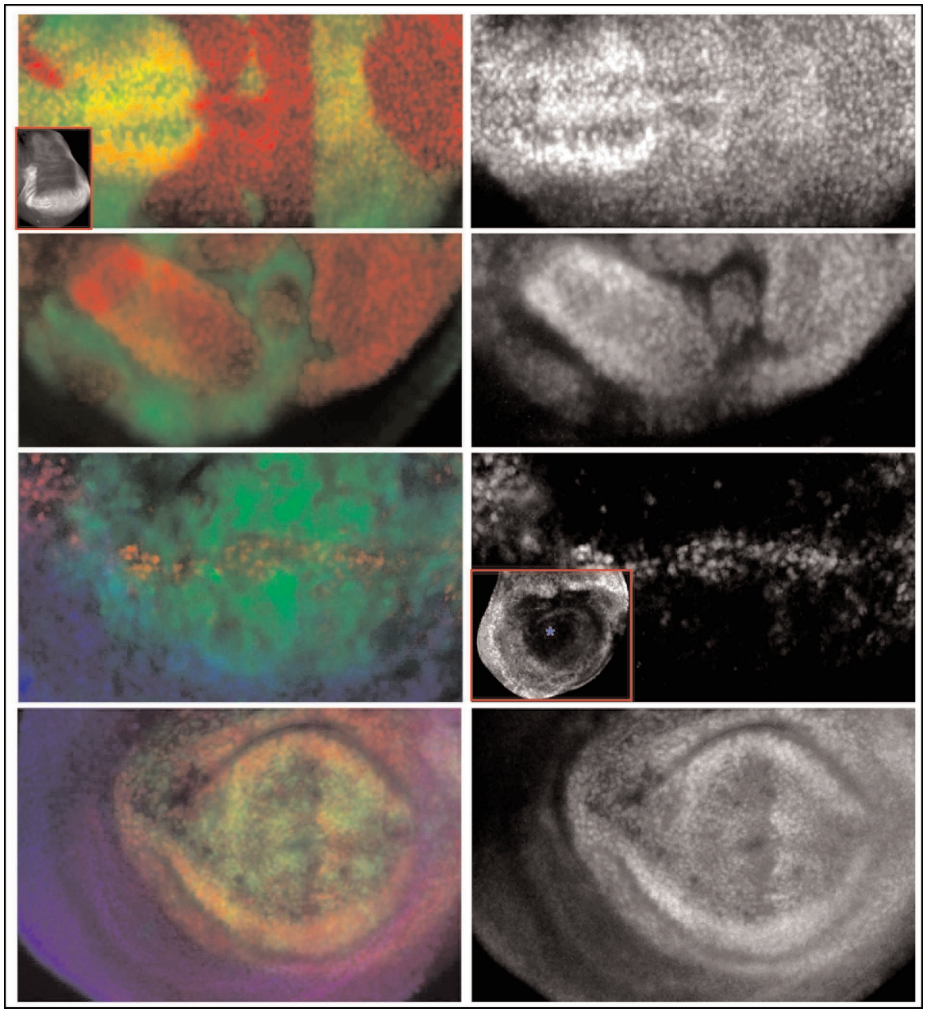

Figure S1 Cells expressing dTcf^{DN} and P35 retain wing cell fates **a,** WP region from a control wing disc with clones of cells expressing GFP and P35. By itself, P35 does not affect Vg expression. Inset shows Vg expression in an entire wing disc. **b**, Clones of cells co-expressing GFP, dTcf^{DN} and P35 lose expression of Vg (arrow). **c**, WP region of a wing disc expressing dTcf^{DN} and P35 throughout the WP. Vg is lost in all cells that express dTcf^{DN} except for those at the DV boundary (where expression due to input from Notch). GFP marks the Gal4 expression domain. Expression of the hinge cell fate marker, Homothorax, (inset and blue in **c**) is still excluded from wing pouch cells expressing dTcf^{DN} and P35 with a WP-specific Gal4 driver, as is Teashirt (Tsh, not shown). **d,** Nubbin (Nub) is expressed normally in the WP of discs expressing dTcf^{DN} and P35. The WP regions of these discs are convoluted, as illustrated by the vertical stripe of Nub-positive nuclei that are out of the plane of focus. Expression of P35 alone did not affect the expression of any of the cell fate markers. The WP driver, C765 was used in **c-d** (see Fig. 5**i** for pattern).

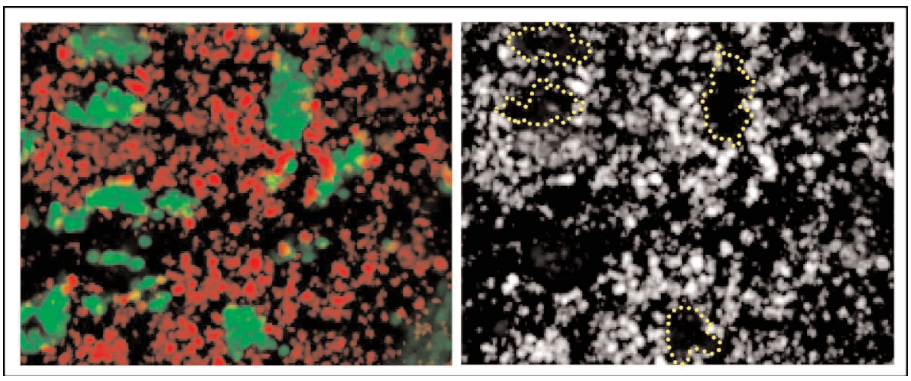

Figure S2 Small Arm* clones lose dE2f1 activity **a, a',** dE2f1 activity in small clones of cells expressing Arm* in the wing pouch. These clones were induced in the early third instar and allowed to grow for approximately 40 hours. While most of the dE2F activity is lost in cells within the clones, occasionally, low levels of dE2f activity can be detected in some cells.